Life Sciences 221 (2019) 249–258

Contents lists available at ScienceDirect

Life Sciences

journal homepage: www.elsevier.com/locate/lifescie

AIM2 gene silencing attenuates diabetic cardiomyopathy in type 2 diabetic rat model

Xuyang Wang[a], Jinyu Pan[b], Hui Liu[a], Mingjun Zhang[a], Dian Liu[a], Lu Lu[c], Jingjing Tian[a], Ming Liu[a], Tao Jin[a], Fengshuang An[a,*]

[a] The Key Laboratory of Cardiovascular Remodeling and Function Research, Chinese Ministry of Education, Chinese National Health Commission and Chinese Academy of Medical Sciences, The State and Shandong Province Joint Key Laboratory of Translational Cardiovascular Medicine, Department of Cardiology, Qilu Hospital of Shandong University, Jinan, China

[b] Department of Cardiology, Shandong Provincial Qianfoshan Hospital of Shandong University, Jinan, Shandong 250012, China

[c] Jinan No. 4 People's Hospital, No. 50, Shifan Road, Jinan, Shandong 250031, China

ARTICLE INFO

Keywords:
AIM2
Diabetic cardiomyopathy
Cell death
ROS
GSDMD

ABSTRACT

Aims: Absent in melanoma 2 (AIM2) is a cytosolic DNA sensor which plays an important role in inflammasome formation and is involved in various cellular functions including pyroptosis, fibrosis, and tissue injury. Our study aimed to investigate whether AIM2 plays a role in diabetic cardiomyopathy (DCM) and to explore its potential molecular mechanism.

Main methods: Sprague-Dawley rats were randomly divided into 4 groups: Control, Diabetes Mellitus (DM), DM + shAIM2, and DM + shNC. The cardiac function of rats was measured. Hematoxylin and eosin staining, Masson's staining, sinus red staining, and immunohistochemistry were performed. H9c2 cardiomyocytes were cultured in DMEM and stimulated with high-glucose treatment (25 mmol/l). The level of reactive oxygen species (ROS) was measured. AIM2-siRNA were used to inhibit the expression of AIM2. TUNEL assay and EthD-III staining were used to measure cell death. The expression levels of AIM2, ASC, caspase-1, IL-1β, and GSDMD-N were measured by western blotting.

Key findings: In the streptozotocin-induced diabetic rat model, AIM2 expression was significantly increased in heart tissue compared with the control. Also, diabetic rats exhibited severe left ventricular dysfunction including metabolic disorder, cardiac fibrosis, and cardiomyocyte death. Gene silencing of AIM2 alleviated cardiac dysfunction which resulted from metabolic disorder and ventricular remodelling. In vitro, treatment of H9C2 cardiomyoblasts with HG significantly increased AIM2, while ROS inhibition reduced the level of AIM2. AIM2-siRNA alleviated GSDMD-N–related pyroptosis in H9c2 cardiomyoblasts.

Significance: Our results indicate that AIM2 plays an important role in cell death and fibrosis in HG-induced, ROS-mediated diabetic cardiomyopathy via the GSDMD pathway.

1. Introduction

Diabetic cardiomyopathy (DCM) is characterized by structural and functional abnormalities of the ventricular myocardium in diabetic patients, which are independent of coronary artery disease or hypertension [1,2]. Reactive oxygen species (ROS) mediated by chronic hyperglycaemia plays a vital role in the pathophysiological progression of and tissue injury in DCM. The increased generation of ROS activates a series of cytokines and inflammatory-related factors which promote both cardiomyocyte death and fibrosis in the development of DCM [3,4]. The inflammasome is one of the target inflammatory factors. Although it has been reported that the inflammasome is involved in the pathogenic progression of diabetes [5], the role and potential mechanism of absent in melanoma 2 (AIM2)-related inflammasome activity in DCM remains unclear.

AIM2, a member of the HIN200 protein family, is a component protein which activates inflammasomes in the presence of DNA or particular stimuli [6–8]. Upon activation, AIM2 is capable of forming a platform with the apoptosis speck like protein (ASC) and activates serine protease caspase-1, further leading to the maturation of IL-1β

* Corresponding author at: The Key Laboratory of Cardiovascular Remodeling and Function Research, Chinese Ministry of Education, Chinese National Health Commission and Chinese Academy of Medical Sciences, The State and Shandong Province Joint Key Laboratory of Translational Cardiovascular Medicine, Department of Cardiology, Qilu Hospital of Shandong University, No. 107, Wenhua Xilu, Jinan 250012, China.

E-mail address: fengshuang.an@hotmail.com (F. An).

https://doi.org/10.1016/j.lfs.2019.02.035
Received 29 January 2019; Received in revised form 15 February 2019; Accepted 16 February 2019
Available online 18 February 2019

and IL-18 which function as mediators of apoptosis and the immune system [9,10].

In addition to their IL-1β pro-maturation roles, inflammatory caspases (caspase-1, -4, -5 and -11) can also be involved in pyroptotic cell death [11]. Pyroptosis, a form of programmed cell death dependent on the cleavage of gasdermin D (GSDMD) by caspase-1 [12,13], presents unique morphological characteristics including DNA fragmentation, perforation of the cell membrane, and the release of pro-inflammatory factors, which are involved in both apoptosis and necrosis [14,15]. Recent studies indicate that pyroptosis promotes cardiomyocyte death stimulated by hyperglycaemia [16]. One area that needs more investigation, however, is the connection between the AIM2 inflammasome and cell death in diabetic cardiomyopathy.

With that background in mind, in this study, we hypothesized that the AIM2 inflammasome participates in the pathogenesis of DCM. Accordingly, we investigated the mechanism and effects of pyroptosis as mediated by the AIM2 inflammasome in H9c2 cardiomyoblasts and in a rat model of diabetic cardiomyopathy.

2. Results

2.1. Basic characteristics of type 2 diabetic rats

After 4 weeks of high-fat diet (HF; 34.5% fat, 17.5% protein, and 48% carbohydrate), the mean area under the receiver operating characteristic curve (AUC) for intraperitoneal glucose tolerance test (IPGTT) and intraperitoneal insulin tolerance test (IPITT) was higher for HF diet rats than the controls ($P < 0.05$, Fig. 1A–D). After 20 weeks of diabetes, diabetic rats showed significantly higher fasting blood glucose (FBG), total cholesterol (TC), triglycerides (TG) levels, insulin tested at the end of the experiment (INS) and insulin sensitivity index (ISI). ($P < 0.05$, Table 1). AIM2 inhibition had no effect on the TC, TG, FBG, ISI and INS ($P > 0.05$, Table 1). The AUC for IPITT and IPGTT was not lower significantly in rats with the inhibition of AIM2 than in vehicle treated animals ($P > 0.05$, Fig. 1E–H).

2.2. Diabetes activated the expression of myocardial AIM2 and AIM2 inhibition attenuated myocardial remodelling in diabetic rats

We found that AIM2 protein levels were significantly increased in rats in the DM group compared with those in the control group. We also found that AIM2-shRNA inhibition downregulated the diabetes-induced increase in expression of AIM2 ($P < 0.05$; Fig. 2A). Additionally, the ratio of heart weight to body weight increased in the DM group compared with the control group (Fig. 2C). The DM group also showed eccentric ventricular hypertrophy and higher cardiomyocyte widths compared with those in the control group, but were alleviated by AIM2-shRNA treatment (Fig. 2B and D). These results indicate that AIM2 inhibition attenuates cardiac remodelling in DM rats.

2.3. AIM2 inhibition improved the cardiac dysfunction caused by diabetes

Echocardiography assessment was performed 4 weeks after AIM2-shRNA transfection. Compared with the control group, DM rats revealed cardiac dysfunction, which manifested as lower LVEF, FS, E/A ratio, and e′/a′ ratio (all $P < 0.05$; Fig. 3B1–B4). In addition, LVEDD and the E/e′ ratio were significantly increased ($P < 0.01$ and $P < 0.05$, respectively; Fig. 3B5–B6). The results showed that AIM2-shRNA improves cardiac dysfunction compared with the DM and DM + NC groups (Fig. 3A,B).

2.4. AIM2 inhibition prevented myocardial fibrosis induced by diabetes

Masson's trichome and Sirius red staining of heart tissue indicated that diabetic myocardium appeared to have higher deposits of extracellular matrix compared with controls, but was alleviated by shRNA treatment (Fig. 4A). Additionally, diabetic animals exhibited overexpression of collagen I and collagen III compared with the control, and AIM2 inhibition significantly reduced the levels of both proteins (Fig. 4B,C). Also, the elevated levels of MMP2 and MMP9 were inhibited through shRNA-AIM2 transfection in DM rats compared with the control group (Fig. 4D). These results demonstrate that AIM2 inhibition prevents diabetic-induced myocardial fibrosis.

2.5. AIM2 gene silencing protects cardial cells from death

The proportion of TUNEL-positive cells was significantly increased in DM cardial tissue, but AIM2-shRNA treatment alleviated this phenomenon (Fig. 5C). Additionally, the protein levels of AIM2 inflammasome, caspase-1, and GSDMD were all increased in the DM group, but were downregulated by AIM2 inhibition (Fig. 5A and B).

2.6. AIM2 expression was increased after HG treatment in H9c2 cardiomyoblasts

The AIM2 protein levels of H9c2 cells treated in DMEM with 5.5 mM glucose (control group, NG) and DMEM with 25 mM glucose (high-glucose control, HG) for 6, 12, 24, and 48 h presented with significant differences (Fig. 6A). Also, H9c2 cardiomyoblasts were cultured with DMEM media containing 5.5, 11.1, 22.2, or 33.3 mM glucose for 24 h. The protein expression of AIM2 significantly increased after being treated with HG concentrations (Fig. 6B). The results demonstrate that HG stimulation promotes the expression of AIM2.

2.7. ROS mediated AIM2 expression with HG stimulation

Because ROS production was increased by HG (Fig. 7A), we investigated the potential mechanism of HG stimulation of AIM2 in H9c2 cells. For this, we used NAC, a ROS inhibitor to inhibit the production of ROS. We found that the expression of AIM2 in the HG + NAC group was significantly downregulated compared with that in the HG group (Fig. 7D).

2.8. AIM2 was involved in HG-induced pyroptotic cell death

Finally, we investigated whether AIM2 is involved in HG-induced cell death. After inhibiting AIM2 expression using AIM2-shRNA lentivirus, the protein level of AIM2 was decreased in HG-stimulated H9c2 cardiomyoblasts. The efficiently inhibited AIM2 also decreased the levels of activated caspase-1 and mature IL-1β compared with the HG group. In addition, the expression of GSDMD decreased significantly in the AIM2-siRNA transfected HG group compared with the HG control group (Fig. 8C). TUNEL and EthD-III staining indicated that HG promoted DNA fragmentation and pyroptotic cell death in H9c2 cardiomyoblasts. For the interference of lentivector fluorescence, we omitted the Calcein AM in order to detect live cells and replaced them using DAPI for total cells. From the results, AIM2 inhibition reduced the proportion of TUNEL positive cells and EthD-III positive cells compared with the HG group (Fig. 8A–B and D–E).

3. Discussion

Diabetic cardiomyopathy, as characterized by left ventricular dysfunction independent of coronary disease and hypertension [1,2], is a major cause of heart failure in patients with diabetes [17]. In this study, we successfully induced a type 2 diabetic model in Sprague-Dawley rats that showed severe metabolic disorder, increased myocardiocyte death and fibrosis, and ultimately cardiac dysfunction. Our study found that the levels of the AIM2 inflammasome and IL-1β in cardiac tissues of diabetic rats were significantly elevated. Interestingly, when we silenced the expression of AIM2, the cardiac function of diabetic rats improved, suggesting that AIM2 plays an important role in the

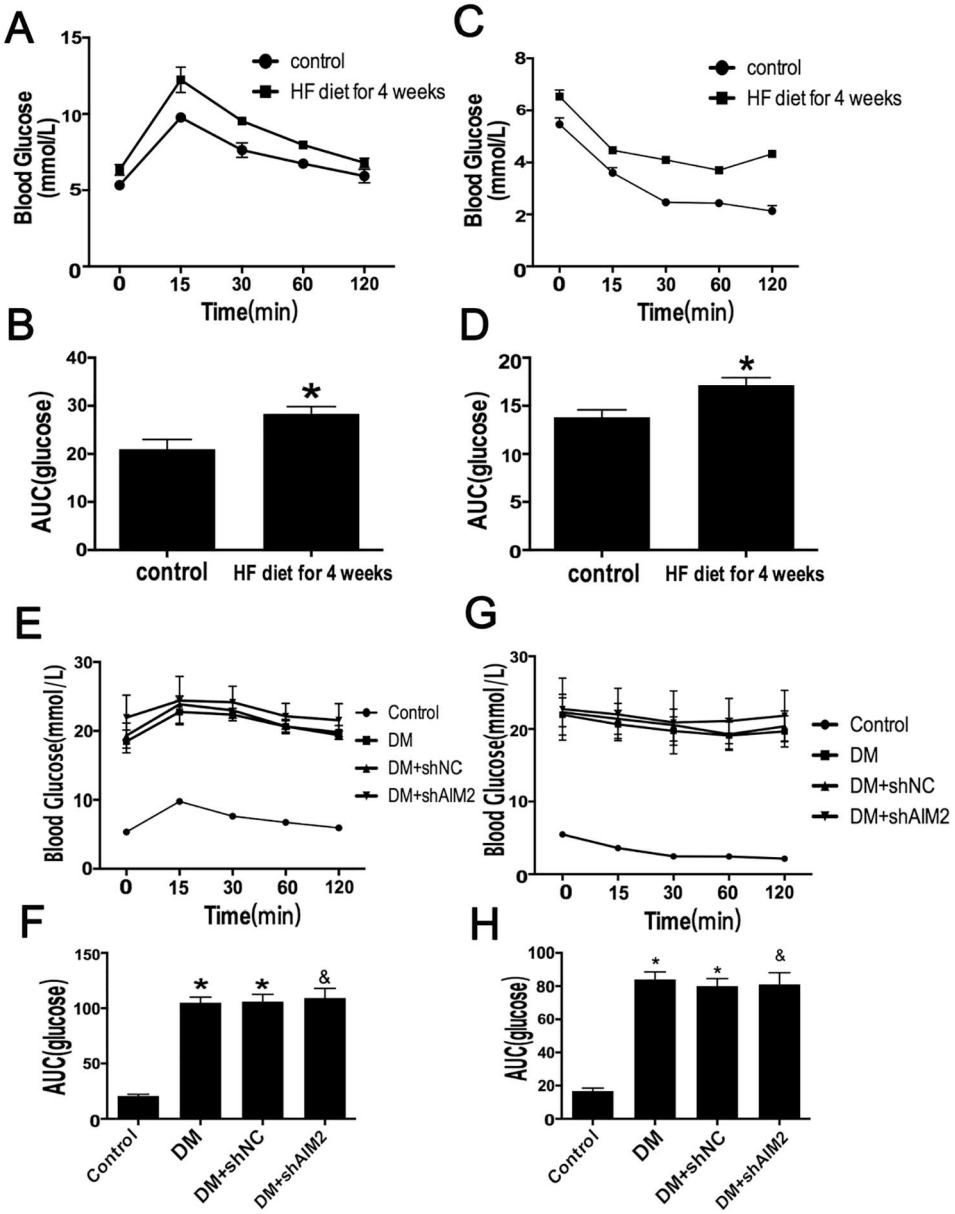

Fig. 1. Blood glucose and level of Insulin reactivity in rats A. and B. Blood level at the control and rats with high fat (HF) diet for 4 weeks; C. and D. Blood level at the control and rats with high fat (HF) diet for 4 weeks; E. and F. Blood level at control and rats at 20 weeks after diabetes. G. and H. Blood level at control and rats at 20 weeks after diabetes. Control: normal rats, DM: diabetic rats, shAIM2: AIM2 shRNA. shNC: negative control shRNA. Data are means ± SD. *P < 0.05 vs control. & P > 0.05 vs the DM or the DM + shNC.

progression of DCM. Therefore, we concluded that AIM2 may be activated in diabetic rats and promote the progression of DCM.

In our study, diabetic rats showed severe metabolic disorders, which is consistent with previous studies [18]. However, by monitoring the changes in blood glucose in the AIM2 gene silencing model of rats, we found that AIM2 had little effect on relieving systemic metabolic

Table 1
Basic information and metabolic index in four groups. SBP: systolic blood pressure. DBP: diastolic blood pressure. MBP: mean blood pressure. FBG: fasting blood glucose. TC: total cholesterol. TG: Triglyceride. INS: insulin tested at the end of the experiment. ISI: insulin sensitivity index. Control: normal rats. DM: Diabetic cardiomyopathy. shAIM2: AIM2 shRNA. shNC: negative control shRNA. N = 6 per group. Data are means ± SD. *P < 0.05 vs control.

	Control	DM	DM + shNC	DM + shAIM2
SBP (mm Hg)	116.7 ± 3.8	123.7 ± 4.1	119.3 ± 4.5	119.6 ± 5.3
DBP (mm Hg)	91.5 ± 4.3	92.4 ± 2.8	93.4 ± 5.9	91.6 ± 3.5
MBP (mm Hg)	99.4 ± 2.5	102.9 ± 4.8	101.7 ± 3.4	103.8 ± 2.4
FBG (mmol/L)	6.09 ± 0.36	21.10 ± 0.81*	20.20 ± 0.38*	22.13 ± 0.62*
TC (mmol/L)	1. 63 ± 0.08	2.89 ± 0.05*	2.81 ± 0.09*	2.92 ± 0.04*
TG (mmol/L)	0.58 ± 0.03	2.73 ± 0.06*	2.76 ± 0.08*	2.71 ± 0.04*
INS (mmol/L)	14.05 ± 0.32	16.17 ± 0.43*	16.34 ± 0.38*	16.09 ± 0.29*
ISI (mmol/L)	−3.88 ± 0.04	−5.21 ± 0.05*	−5.27 ± 0.02*	−5.36 ± 0.08*

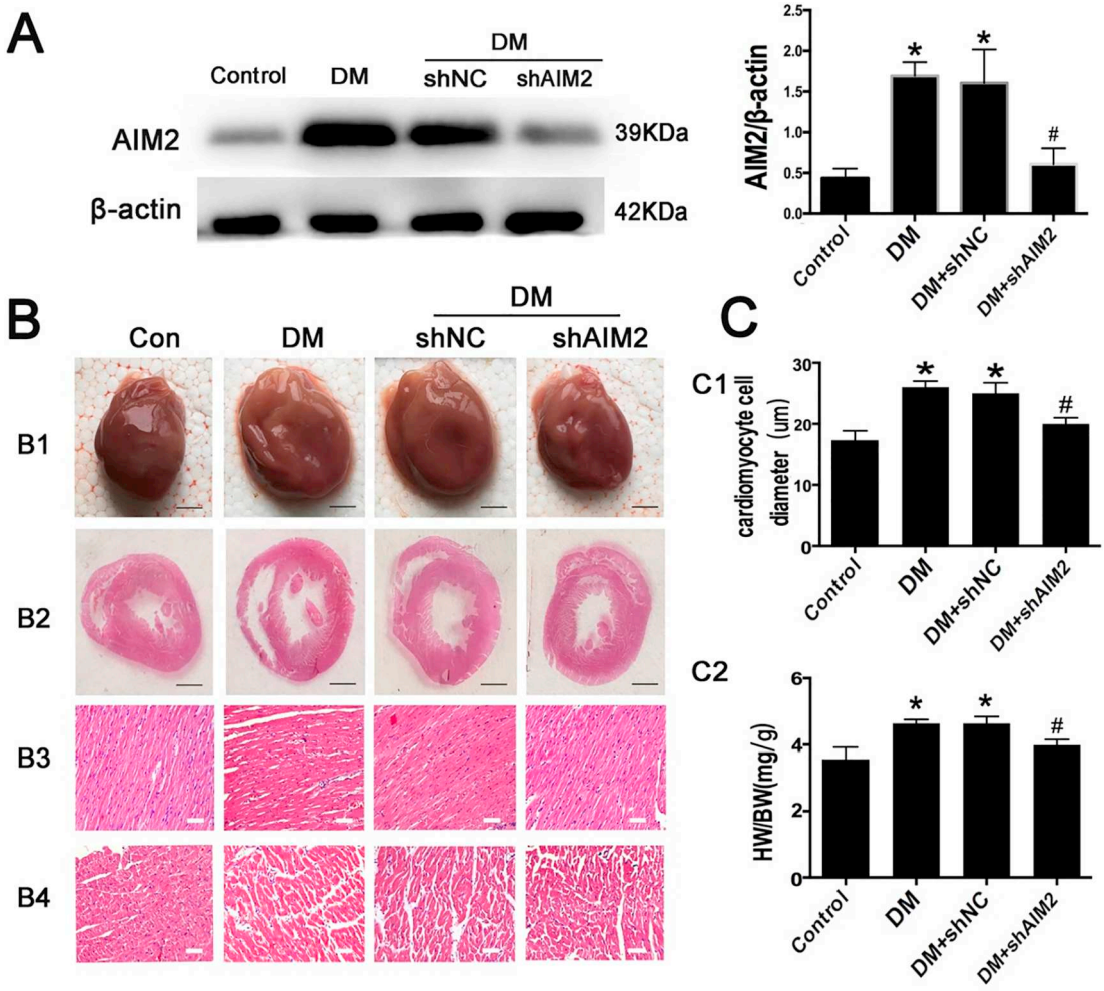

Fig. 2. AIM2 expression and myocardial pathology in vivo. A: Western blot analysis of AIM2 expression in heart tissue. B1: Heart size (scale bar: 3 mm). B2: histological sectional image at the papillary level (scale bar: 3 mm). B3 and B4: hematoxylin and eosin staining (HE) of longitudinal and transverse left ventricle (LV) section (scale bar: 20 μm). C1: Quantitative analysis of cardiomyocyte cell diameter. C2: heart weight/body weight (mg/g). Con or Control: normal rats. DM: Diabetic cardiomyopathy. shAIM2: AIM2 shRNA. shNC: negative control shRNA. Data are means ± SD. *P < 0.05 vs the control. #P < 0.05 vs the DM or the DM + shNC.

disorders. Therefore, we concluded that the role of the AIM2 inflammasome in DCM was not through systemic effects.

Under diabetic conditions, proinflammatory cytokines induced by hyperglycaemia can lead to a persistent inflammatory state in myocardial tissue and promote functional disorders of the heart [19,20]. Our previous study found that NLRP3 is involved in the pathological progression of DCM [21], and the present study demonstrated that AIM2 inhibition treatment can also alleviate the inflammatory response of DCM by reducing the levels of ASC, caspase-1, and IL-1β.

In addition to its pro-inflammatory effects, AIM2 also plays an important role in pyroptosis [22,23] which is a type of inflammatory programmed cell death that is dependent on caspase-1 [13,14]. The perforation of the membrane in the early stage of pyroptosis promotes the secretion of protein in cells, which results in the initiation of cellular rupture caused by swelling of the cytoplasm [22,23]. Also, the initiation of pyroptosis can lead to DNA damage in the nucleus [24]. Previous studies on myocardial cell death in DCM mainly focused on the effects of apoptosis [20,25], but there has been less research conducted on the role of pyroptosis [26]. Recent studies have shown that pyroptosis plays an important role in the progression of diabetic cardiomyopathy andNLRP3, microRNA-9, and microRNA-30d regulate the levels of pyroptosis in DCM [27–29]. As an innate immune receptor, AIM2 was originally localized in human melanoma cells [30]. Recent studies have shown that the inhibition of AIM2 in macrophages activates pyroptosis [31]. Previous studies have also found that AIM2 can bind directly to and is activated by dsDNA [32]. Activated AIM2 can promote the recruitment of the inflammasome and further activates GSDMD-N. In this study, we found that the level of GSDMD-N, an enzyme that plays an important role in pyroptosis [33], decreased after AIM2 gene silencing, and the progression of diabetic cardiomyopathy was reduced. At the same time, we found that the level of AIM2 increased in H9c2 cells treated with HG. Furthermore, we demonstrated that AIM2 gene silencing reduced the level of GSDMD-N in in vitro experiments. Also, EthD-III and TUNEL staining showed that AIM2 gene silencing can indeed reduce the level of pyroptosis in H9c2 treated with HG.

Previous studies have shown that oxidative stress induced by HG is closely related to the progression of DCM [3,4]. As the production of ROS increases, the level of oxidative stress is elevated under HG conditions. Overexpression of ROS can lead to myocardial fibrosis and cell death [34,35]. Our study found that ROS overexpression was induced by HG in H9c2 cardiomyocytes and was related to the concentration of glucose. Interestingly, this process was accompanied by an increase of AIM2. After inhibition of ROS, the level of AIM2 dropped in H9c2 cardiomyocytes treated with HG. So, we determined that oxidative stress may regulate the expression of AIM2 in H9c2 cardiomyocytes treated with HG.

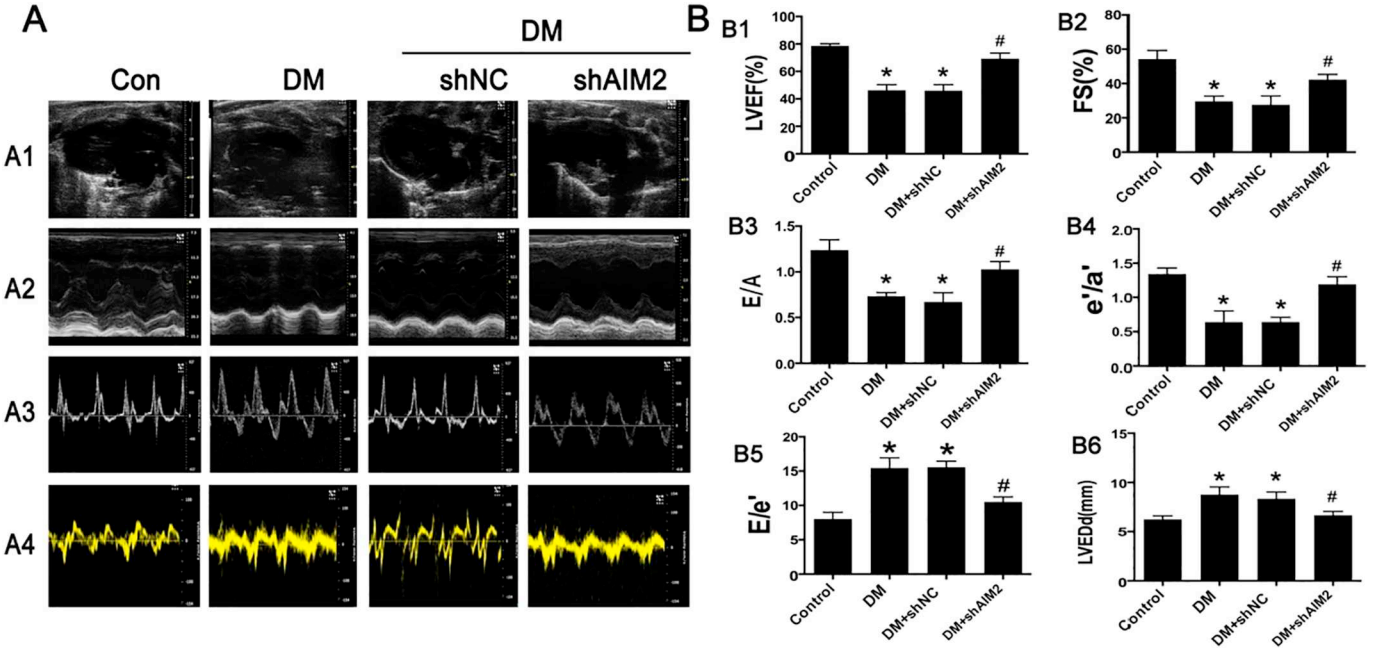

Fig. 3. Cardiac function in rats measured by echocardiography. A1: representative 2D echocardiograms. A2: representative M-mode echocardiograms. A3: representative pulse-wave Doppler echocardiograms of mitral inflow. A4: representative tissue Doppler echocardiograms. B1: Left ventricle ejection fraction (LVEF). B2: Fractional shortening (FS). B3: Early to late mitral flow (E/A). B4: Ratio of diastolic mitral annulus velocities (e'/a'). B5: E/e'. B6: Left ventricle end-diastolic dimension (LVEDd). Con or Control: normal rats. DM: Diabetic cardiomyopathy. shAIM2: AIM2 shRNA. shNC: negative control shRNA. Data are means ± SD. *P < 0.05 vs the control. #P < 0.05 vs the DM or the DM + shNC.

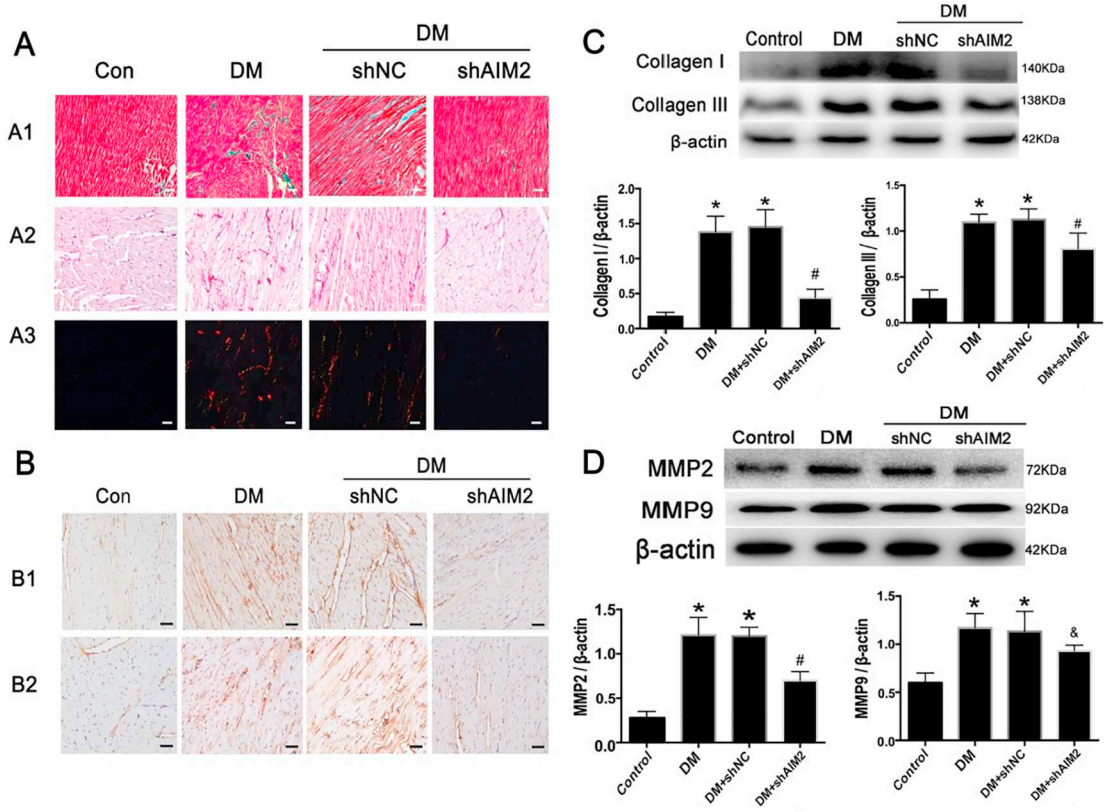

Fig. 4. Effect of AIM2 on collagen deposition in vivo. A1: Masson staining. A2 and A3: Picrosirius red staining of myocardium. B1 and B2: Immunohistochemical staining of collagen I and collagen III. C: Western blot analysis of the protein expression of collagen I and collagen III. Scale bar: 50 μm. D: Western blot analysis of the protein level of MMP2 and MMP9. Con or Control: normal rats. DM: Diabetic cardiomyopathy. shAIM2: AIM2 shRNA. shNC: negative control shRNA. Data are means ± SD. *P < 0.05 vs the control. #P < 0.05 vs the DM or the DM + shNC.

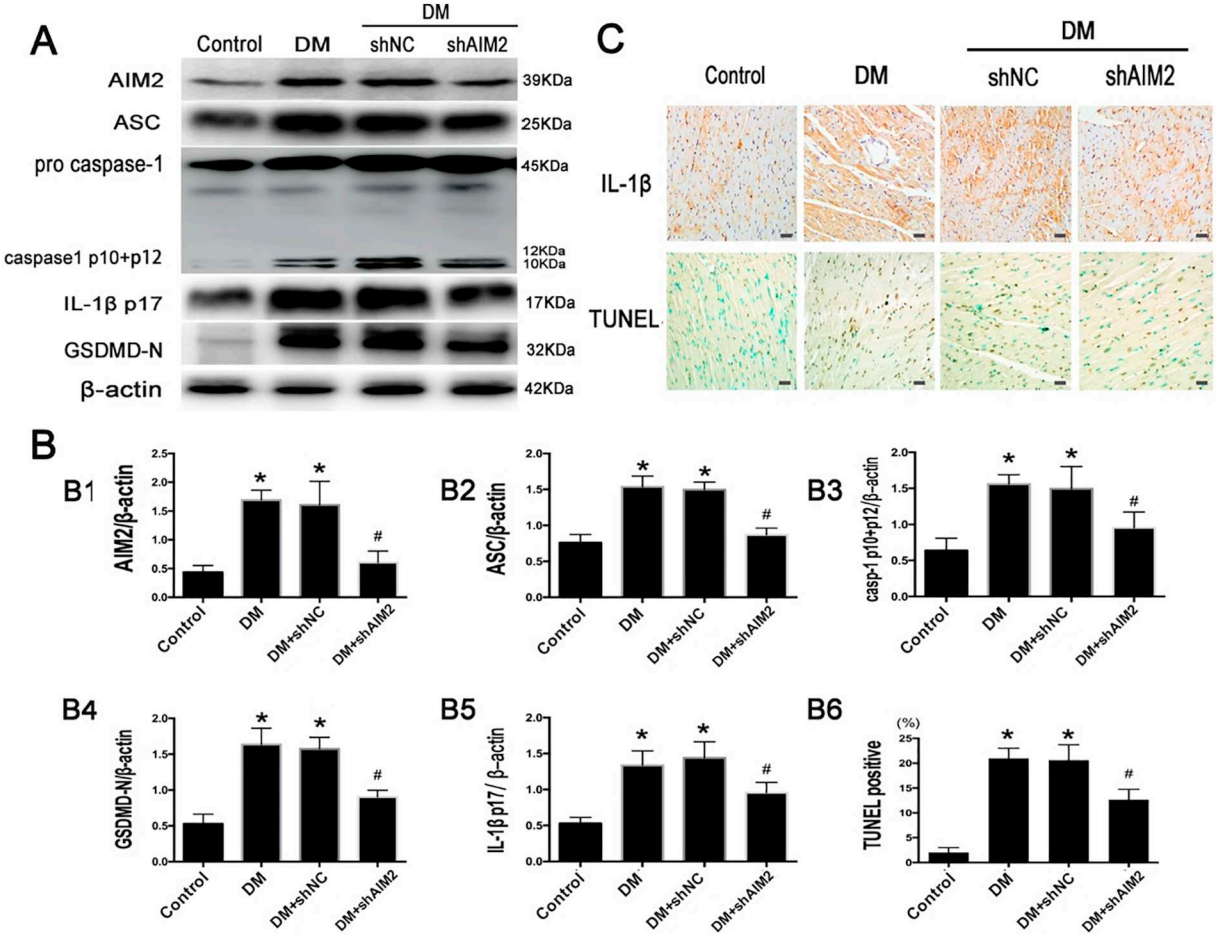

Fig. 5. Role of AIM2 inflammasome in myocardial cell death in vivo. A-B5: Western blot analysis for the protein expression of AIM2 (B1), ASC (B2), caspase p10 and p12 (B3), IL-1β (B4), and GSDMD-N (B5). B6: Quantitative analysis of TUNEL positive cells. C: Immunohistochemical staining of IL-1βand TUNEL staining. Scale bar: 50 μm. Con or Control: normal rats. DM: Diabetic cardiomyopathy. shAIM2: AIM2 shRNA. shNC: negative control shRNA. Data are means ± SD. *P < 0.05 vs the control. #P < 0.05 vs the DM or the DM + shNC.

4. Materials and methods

4.1. Animals

60 Sprague-Dawley rats (100–120 g) were randomly divided into 4 groups (n = 15). All rats were kept in a 23 °C environment with light-dark cycles. The control group was fed a basal diet while the other 3 groups were fed a high fat diet (HF diet: 16% fat and 0.30% cholesterol). Animals were fed the HF diet for 4 weeks, and intraperitoneal insulin tolerance test (IPITT) and intraperitoneal glucose tolerance test (IPGTT) were conducted to identify insulin-resistant rats. To induce diabetes in the identified insulin-resistant rates, a single intraperitoneal injection of streptozotocin (STZ: 40 mg/kg, Beijing Solarbio, Beijing, China) was administered. Then, 7 days after injection, the fasting blood

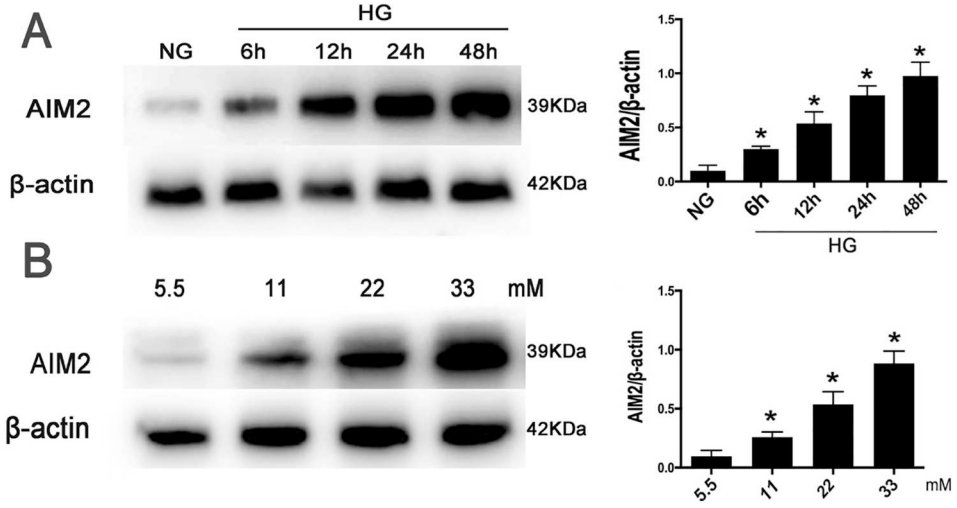

Fig. 6. High glucose induced AIM2 expression in H9c2 cardiomyocytes. A: Western blot analysis of the protein expression of AIM2 in different glucose concentration in H9C2 cardiomyocyte. B: Western blot analysis of the protein expression of AIM2 in different HG culture time in H9C2 cardiomyocyte. NG: 5.5 mM. HG: 25 Mm. Data are means ± SD. *P < 0.05 vs NG.

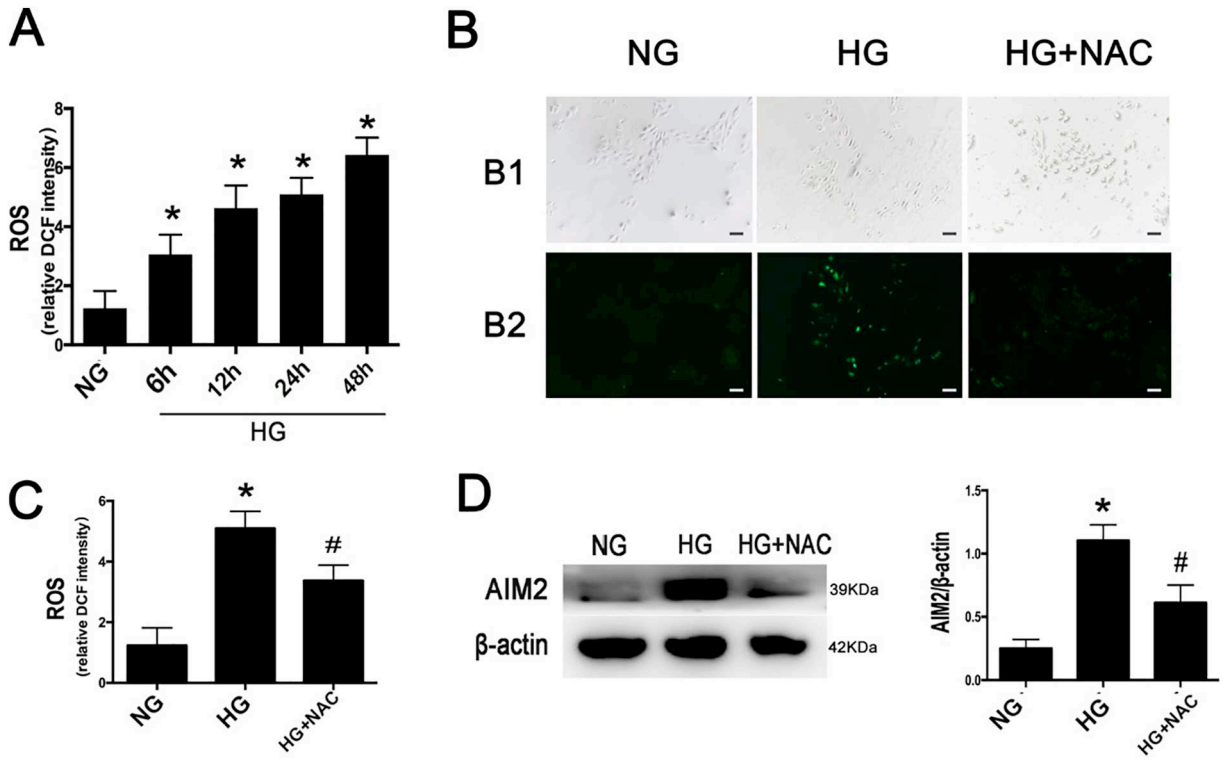

Fig. 7. Effect of increasing ROS on AIM2 in H9C2 cardiomyocyte. A: The effect of high glucose on ROS. B and C: The level of ROS in NAC inhibition. B1: The bright field. B2: immunofluorescence staining of ROS. Scale bar: 50 μm. D: Western blot analysis of AIM2 after ROS inhibition. NG: 5.5 mM. HG: 25 Mm. Data are means ± SD. *P < 0.05 vs NG.

glucose (FBG) level was measured. Only rats with FBG of ≥11.1 mmol/L were considered as being a successful diabetic model [36]. After 8 weeks of STZ injection, rats were administered either AIM2-shRNA or NC-shRNA through a local injection in the heart with a concentration of 1×10^8. The sequence of AIM2-shRNA was: 5′-GGTCACCAGTTCCTCA GTT-3′. The negative control (NC) sequence of shRNA was: 5′-TTCTC CGAACGTGTCACGT-3′. The transcription efficiency was judged 2 weeks after shRNA injection using a fluorescence microscope. All rats were sacrificed 4 weeks after injection of the shRNA virus. All experimental protocols were approved by the Shandong University Animal Care Committee.

4.2. Cardiac function

The cardiac function of rats was measured using the Vevo 770 imaging system with RMB710 transducer (VisualSonics, Toronto, Canada). The echocardiography parameters for assessing cardiac function were as follows: left ventricular end-diastolic dimension (LVEDD), left ventricular ejection fraction (LVEF), peak E to peak A ratio (E/A), early (e′) to late (a′), diastolic velocity ratio (e/a), peak E to early (e′) ratio (E/e′), and fractional shortening (FS).

4.3. Histology staining

After the rats were sacrificed, heart tissue was dissected, fixed with 4% paraformaldehyde, and embedded in paraffin, which were then sliced into 4 μm sections for hematoxylin and eosin staining. We performed Masson's trichrome and sinus red staining to measure the level of fibrosis. We used the following antibodies for immunohistochemistry: collagen III (NB600-594SS, Novus Biologicals), collagen I (NBP1-30054, Novus Biologicals), IL-1β (ab200478, Abcam), and AIM2 (ab180665, Abcam). Briefly, the collagen I and collagen III primary antibodies were incubated with tissue sections overnight at 4 °C and then, tissue sections were washed with phosphate buffered saline (PBS) and incubated in a secondary antibody for 30 min in 37 °C [37].

4.4. Cell treatment

Primary cardiomyocytes were extracted from neonatal rat ventricular tissue. Primary or H9c2 cardiomyocytes were plated in 6-well plates (Corning Inc., Corning, NY) with Dulbecco's modified Eagle's medium (DMEM, glucose 5.5 mM) supplemented with 10% foetal bovine serum (FBS) and 1% penicillin- streptomycin at 37 °C in 5% CO_2 for > 12 h. When the cells reached 60% confluence, minimal essential medium was substituted with media containing different glucose concentrations (glucose: 11.1 mM, 22.2 mM, 33.3 mM). The osmotic pressure was balanced by mannitol and stimulated for 24 h. Cells were treated with HG, (25 mM) for 6, 12, 24, and 48 h or with low glucose (LG, 5.5 mM) which was used as a control [38]. In the ROS-related experiment, 5 mmol/L *N*-acetylcysteine (NAC, Beyotime, Beijing, China) was used to inhibit ROS at the time of HG stimulation for 24 h [38].

4.5. siRNA transfection

AIM2-siRNA (JiMa, Shanghai, China) was transfected into H9c2 cardiomyocytes 24 h prior to stimulation with lipofectamine 2000 (Invitrogen, Carlsbad, CA) in medium. The sequence with the highest AIM2-siRNA transfection efficiency was GGUACCAGUUCCUCAGUUTT.

4.6. ROS levels

The level of intracellular ROS was measured using a peroxide-sensitive fluorescent probe 2′,7′-diacetate (Sigma-Aldrich, Shanghai, China). Fluorescence microscopy (488-nm filter, Olympus, Tokyo, Japan) was used to detect the fluorescent signal of 5 fields per pore. HMIAS-2000 software was used to analyse the intensity [39].

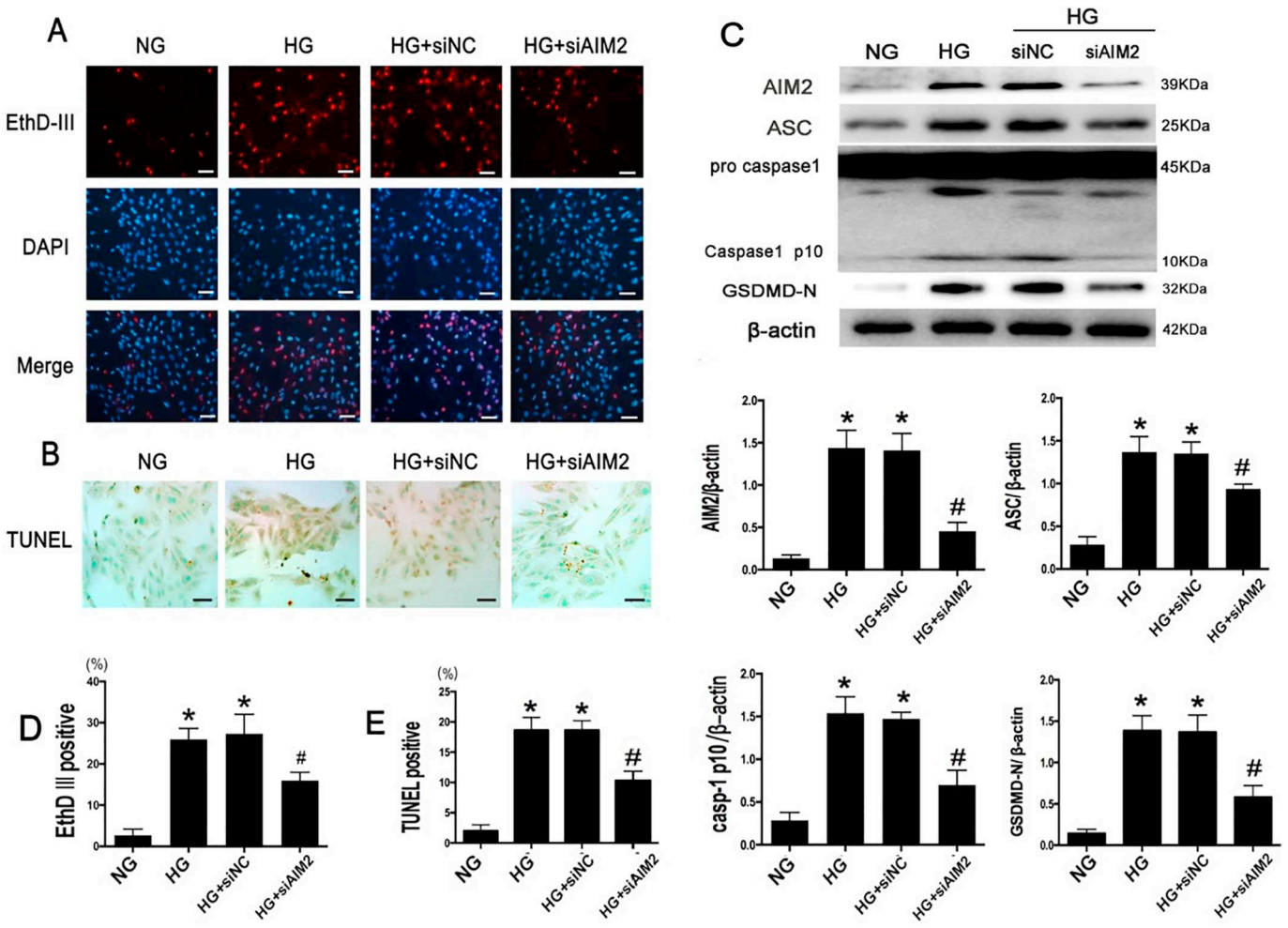

Fig. 8. AIM2 induced GSDMD-N expression and pyroptosis in H9c2 cells. A: EthD-III staining of H9c2 cells. Scale bar: 50 μm B: TUNEL staining of H9c2 cells. Scale bar: 20 μm C: Western blot analysis of AIM2 (C2),ASC (C3),Caspase1 p10 (C4), GSDMD-N (C5). D: ratio of EthD-III positive cell. E: ratio of TUNEL positive cell. NG: 5.5 Mm. HG: 25 Mm. siAIM2: AIM2 siRNA. siNC: negative control siRNA. Data are means ± SD. *P < 0.05 vs NG. #P < 0.05 vs HG or HG + siNC.

4.7. Cell death assay

To investigate cell death, TUNEL assay and EthD-III staining were used. First, for DNA fragmentation, a TUNEL assay kit (Millipore) was used to treat H9c2 cardiomyoblasts or tissue sections according to the manufacturer's instructions. Briefly, cells were fixed with 4% paraformaldehyde for 10 min at room temperature and then washed twice with PBS. Paraffin tissue sections were treated with 20 μg/ml proteinase K for 5 min. Then the samples were treated with 3% H_2O_2 for 15 min and incubated with 10 μl TdT enzyme reaction buffer for 1 h at 37 °C. After incubation, digoxigenin antibody buffer was added before DAB incubation. PBS was used to wash the residual buffer one last time [40]. Cell death was assessed using the EthD-III/Calcein AM staining kit (Viability/Cytotoxicity Assay Kit, Biotium Inc., Fremont, CA) according to the manufacturer's instructions. Briefly, cells were incubated with 4 μM EthD-III at 37 °C for 30 min and then treated with DAPI staining. Red fluorescence indicated dead cells as EthD-III enters dead cells [41].

4.8. Western blot

Protein from rat heart or from cells was separated by running a 10% SDS-PAGE and then transferring to a polyvinylidene fluoride membrane (Millipore). Five percent non-fat milk was used to block the membrane for 1 h at room temperature and then the protein on the membrane was incubated overnight with the primary antibody at 4 °C. Secondary antibodies were used for 1 h at room temperature and enhanced chemiluminescence (Millipore) was used for exposure via Amersham Imager 600 (General Electric Co., Boston, MA) [42]. We used the following antibodies against AIM2 (ab180665, Abcam), ASC (NBP1-78977SS, Novus Biologicals), pro-IL-1β (ab216995, Abcam), IL-1βp17 (ab216995, Abcam), pro-caspase 1 + p10 + p12 (ab179515, Abcam), GSDMD-N (ab209845, Abcam), collagen III (NB600-594SS, Novus Biologicals), collagen I (NBP1-30054, Novus Biologicals), MMP2 (10373-2-AP, Proteintech, Rosemont, IL), MMP9 (10387-2-AP, Proteintech) and β-actin (ab8227, Abcam) for detection.

4.9. Statistical analysis

All analyses were done in Prism 6.0 (GraphPad) and SPSS 20.0. One-way ANOVA was used to compare the difference among groups and unpaired *t*-tests were used for differences between two groups. Each experiment was repeated at least 3 times and all data is shown as means ± standard deviation. Two-tailed P < 0.05 was regarded as statistically significant.

5. Conclusion

We demonstrated that AIM2 is activated in an HG environment, with the high level of ROS playing a role in the activation of AIM2. Compared with the control group, AIM2 regulated the process of cell death and fibrosis in the heart tissue of diabetic rats, and further influenced cardiac function. This process was alleviated by AIM2 gene

silencing. The in vitro experiment results were consistent with those in the in vivo experiments. We found that the AIM2 inflammasome modulates the expression of the GSDMD-N pathway. The underlying mechanism remains unclear however, and further studies are needed to investigate the effects of AIM2 in the progression of pyroptosis in DCM.

Abbreviations

AIM2	absent in melanoma
DCM	diabetic cardiomyopathy
HG	high glucose
ROS	reactive oxygen species
STZ	streptozocin
IPITT	intraperitoneal insulin tolerance test
IPGTT	intraperitoneal glucose tolerance test
LVEDd	left ventricular end-diastolic dimension
LVEF	left ventricular ejection fraction
E/A	peak E to peak A ratio
e′/a′	early (e′) to late (a′) diastolic velocity ratio
E/e′	peak E to early (e′) ratio
FS	fractional shortening
FBG	fasting blood glucose
HE	hematoxylin and eosin staining
PBS	phosphate buffered saline
NAC	*N*-acetylcysteine

Ethics approval and consent to participate

All experimental protocols related to animals were approved by the Shandong University Animal Care Committee.

Consent for publication

Not applicable.

Availability of data and material

All data generated or analyzed during this study are included in this published article and its additional information files.

Competing interests

The authors declare that they have no competing interests.

Funding

This work was supported by the National Natural Science Foundation of China (grant numbers 81670325 and grant numbers 81370325).

Authors' contributions

F. An and X. Wang was responsible to induce animal model and cell experiment. J. Tian performed immunohistochemistry staining and other staining. D. Liu and M. Zhang analyzed and interpreted the animal model data. L. Lu performed the ultrasonic cardiogram examination of the heart. J. Pan was a major contributor in writing the manuscript. H. Liu carried out western blot experiment. All authors read and approved the final manuscript.

Acknowledgements

The authors thank Yun Zhang for his help in editing the manuscript.

References

[1] D.S. Bell, Diabetic cardiomyopathy, Diabetes Care 26 (2003) 2949–2951.
[2] S. Boudina, E.D. Abel, Diabetic cardiomyopathy revisited, Circulation. 115 (2007) 3213–3223.
[3] A. Faria, S.J. Persaud, Cardiac oxidative stress in diabetes: mechanisms and therapeutic potential, Pharmacol. Ther. 172 (2017) 50–62.
[4] D. Roul, F.A. Recchia, Metabolic alterations induce oxidative stress in diabetic and failing hearts: different pathways, same outcome, Antioxid. Redox Signal. 22 (2015) 1502–1514.
[5] X. Palomer, L. Salvado, E. Barroso, M. Vazquez-Carrera, An overview of the crosstalk between inflammatory processes and metabolic dysregulation during diabetic cardiomyopathy, Int. J. Cardiol. 168 (2013) 3160–3172.
[6] T. Fernandes-Alnemri, J.W. Yu, P. Datta, J. Wu, E.S. Alnemri, AIM2 activates the inflammasome and cell death in response to cytoplasmic DNA, Nature. 458 (2009) 509–513.
[7] K. Schroder, J. Tschopp, The inflammasomes, Cell. 140 (2010) 821–832.
[8] T. Strowig, J. Henao-Mejia, E. Elinav, R. Flavell, Inflammasomes in health and disease, Nature. 481 (2012) 278–286.
[9] M. Hakimi, A. Peters, A. Becker, D. Bockler, S. Dihlmann, Inflammation-related induction of absent in melanoma 2 (AIM2) in vascular cells and atherosclerotic lesions suggests a role in vascular pathogenesis, J. Vasc. Surg. 59 (2014) 794–803.
[10] T.L. Roberts, A. Idris, J.A. Dunn, G.M. Kelly, C.M. Burnton, S. Hodgson, et al., HIN-200 proteins regulate caspase activation in response to foreign cytoplasmic DNA, Science (New York, N.Y.) 323 (2009) 1057–1060.
[11] L. Galluzzi, A. Lopez-Soto, S. Kumar, G. Kroemer, Caspases connect cell-death signaling to organismal homeostasis, Immunity. 44 (2016) 221–231.
[12] T. Bergsbaken, S.L. Fink, B.T. Cookson, Pyroptosis: host cell death and inflammation, Nat. Rev. Microbiol. 7 (2009) 99–109.
[13] J. Shi, W. Gao, F. Shao, Pyroptosis: gasdermin-mediated programmed necrotic cell death, Trends Biochem. Sci. 42 (2017) 245–254.
[14] I. Jorgensen, M. Rayamajhi, E.A. Miao, Programmed cell death as a defence against infection, Nat. Rev. Immunol. 17 (2017) 151–164.
[15] X. Liu, Z. Zhang, J. Ruan, Y. Pan, V.G. Magupalli, H. Wu, et al., Inflammasome-activated gasdermin D causes pyroptosis by forming membrane pores, Nature. 535 (2016) 153–158.
[16] B. Luo, F. Huang, Y. Liu, Y. Liang, Z. Wei, H. Ke, et al., NLRP3 inflammasome as a molecular marker in diabetic cardiomyopathy, Front. Physiol. 8 (2017) 519.
[17] F. Zannad, C.P. Cannon, W.C. Cushman, G.L. Bakris, V. Menon, A.T. Perez, et al., Heart failure and mortality outcomes in patients with type 2 diabetes taking alogliptin versus placebo in EXAMINE: a multicentre, randomised, double-blind trial, Lancet (London, England) 385 (2015) 2067–2076.
[18] Y. Katsuda, T. Ohta, K. Miyajima, Y. Kemmochi, T. Sasase, B. Tong, et al., Diabetic complications in obese type 2 diabetic rat models, Exp. Anim. 63 (2014) 121–132.
[19] B. Feng, S. Chen, A.D. Gordon, S. Chakrabarti, miR-146a mediates inflammatory changes and fibrosis in the heart in diabetes, J. Mol. Cell. Cardiol. 105 (2017) 70–76.
[20] W.D. Qin, G.L. Liu, J. Wang, H. Wang, J.N. Zhang, F. Zhang, et al., Poly(ADP-ribose) polymerase 1 inhibition protects cardiomyocytes from inflammation and apoptosis in diabetic cardiomyopathy, Oncotarget. 7 (2016) 35618–35631.
[21] B. Luo, B. Li, W. Wang, X. Liu, Y. Xia, C. Zhang, et al., NLRP3 gene silencing ameliorates diabetic cardiomyopathy in a type 2 diabetes rat model, PLoS One 9 (2014) e104771.
[22] N.M. de Vasconcelos, N. Van Opdenbosch, H. Van Gorp, E. Parthoens, M. Lamkanfi, Single-cell analysis of pyroptosis dynamics reveals conserved GSDMD-mediated subcellular events that precede plasma membrane rupture, Cell Death Differ. 26 (1) (2019) 146–161, https://doi.org/10.1038/s41418-018-0106-7 (Epub 2018 Apr 17).
[23] L. DiPeso, D.X. Ji, R.E. Vance, J.V. Price, Cell death and cell lysis are separable events during pyroptosis, Cell Death Dis. 3 (2017) 17070.
[24] B.C. Liu, J. Sarhan, A. Panda, H.I. Muendlein, V. Ilyukha, J. Coers, et al., Constitutive interferon maintains GBP expression required for release of bacterial components upstream of pyroptosis and anti-DNA responses, Cell Rep. 24 (2018) (155-68.e5).
[25] X. Hu, T. Bai, Z. Xu, Q. Liu, Y. Zheng, L. Cai, Pathophysiological fundamentals of diabetic cardiomyopathy, Compr. Physiol. 7 (2017) 693–711.
[26] W. Zhou, C. Chen, Z. Chen, L. Liu, J. Jiang, Z. Wu, et al., NLRP3: a novel mediator in cardiovascular disease, J Immunol Res 2018 (2018) 5702103.
[27] P. Jeyabal, R.A. Thandavarayan, D. Joladarashi, S.S. Babu, S. Krishnamurthy, A. Bhimaraj, et al., MicroRNA-9 inhibits hyperglycemia induced cardiac pyroptosis in human ventricular cardiomyocytes by targeting ELAVL1, Biochem. Biophys. Res. Commun. 471 (2016) 423–429.
[28] X. Li, N. Du, Q. Zhang, J. Li, X. Chen, X. Liu, et al., MicroRNA-30d regulates cardiomyocyte pyroptosis by directly targeting foxo3a in diabetic cardiomyopathy, Cell Death Dis. 5 (2014) e1479.
[29] A. Sharma, M. Tate, G. Mathew, J.E. Vince, R.H. Ritchie, J.B. de Haan, Oxidative stress and NLRP3-inflammasome activity as significant drivers of diabetic cardiovascular complications: therapeutic implications, Front. Physiol. 9 (2018) 114.
[30] D. Choubey, Absent in melanoma 2 proteins in the development of cancer, Cell Mol. Life Sci. 73 (2016) 4383–4395.
[31] J.D. Sauer, C.E. Witte, J. Zemansky, B. Hanson, P. Lauer, D.A. Portnoy, Listeria monocytogenes triggers AIM2-mediated pyroptosis upon infrequent bacteriolysis in the macrophage cytosol, Cell Host Microbe 7 (2010) 412–419.
[32] K. Eichholz, T. Bru, T.T. Tran, P. Fernandes, H. Welles, F.J. Mennechet, et al., Immune-complexed adenovirus induce AIM2-mediated pyroptosis in human

dendritic cells, PLoS Pathog. 12 (2016) e1005871.
[33] S. Feng, D. Fox, S.M. Man, Mechanisms of gasdermin family members in inflammasome signaling and cell death, J. Mol. Biol. 12 (9) (2016) e1005871, , https://doi.org/10.1371/journal.ppat.1005871 (eCollection 2016 Sep.).
[34] A.J. Wilson, E.K. Gill, R.A. Abudalo, K.S. Edgar, C.J. Watson, D.J. Grieve, Reactive oxygen species signalling in the diabetic heart: emerging prospect for therapeutic targeting, Heart 104 (2018) 293–299.
[35] Y. Zhao, M. Ponnusamy, Y. Dong, L. Zhang, K. Wang, P. Li, Effects of miRNAs on myocardial apoptosis by modulating mitochondria related proteins, Clin. Exp. Pharmacol. Physiol. 44 (2017) 431–440.
[36] Y. Xia, L. Gong, H. Liu, B. Luo, B. Li, R. Li, et al., Inhibition of prolyl hydroxylase 3 ameliorates cardiac dysfunction in diabetic cardiomyopathy, Mol. Cell. Endocrinol. 403 (2015) 21–29.
[37] S. Korkmaz-Icoz, S. Al Said, T. Radovits, S. Li, M. Brune, P. Hegedus, et al., Oral treatment with a zinc complex of acetylsalicylic acid prevents diabetic cardiomyopathy in a rat model of type-2 diabetes: activation of the Akt pathway, Cardiovasc. Diabetol. 15 (2016) 75.
[38] W. Su, Y. Zhang, Q. Zhang, J. Xu, L. Zhan, Q. Zhu, et al., N-acetylcysteine attenuates myocardial dysfunction and postischemic injury by restoring caveolin-3/eNOS signaling in diabetic rats, Cardiovasc. Diabetol. 15 (2016) 146.
[39] W. Guo, X. Liu, J. Li, Y. Shen, Z. Zhou, M. Wang, et al., Prdx1 alleviates cardiomyocyte apoptosis through ROS-activated MAPK pathway during myocardial ischemia/reperfusion injury, Int. J. Biol. Macromol. 112 (2018) 608–615.
[40] X.M. Wang, Y.C. Wang, X.J. Liu, Q. Wang, C.M. Zhang, L.P. Zhang, et al., BRD7 mediates hyperglycaemia-induced myocardial apoptosis via endoplasmic reticulum stress signalling pathway, J. Cell. Mol. Med. 21 (2017) 1094–1105.
[41] J. Pan, L. Han, J. Guo, X. Wang, D. Liu, J. Tian, et al., AIM2 accelerates the atherosclerotic plaque progressions in ApoE−/− mice, Biochem. Biophys. Res. Commun. 498 (2018) 487–494.
[42] H. Liu, Y. Xia, B. Li, J. Pan, M. Lv, X. Wang, et al., Prolyl hydroxylase 3 overexpression accelerates the progression of atherosclerosis in ApoE−/− mice, Biochem. Biophys. Res. Commun. 473 (2016) 99–106.